PRESTRESSED CONCRETE PAVEMENTS. VOLUME I. DULLES TEST ROAD INSTRUMENTATION AND LOAD TESTS

Eugene C. Odom, et al

Army Engineer Waterways Experiment Station

Prepared for:

Federal Aviation Administration

October 1974

NOTICES

This document is disseminated under the sponsorship of the Department of Transportation in the interest of information exchange. The United States Government assumes no liability for its contents or use thereof.

The United States Government does not endorse products or manufacturers. Trade or manufacturers' names appear herein solely because they are considered essential to the object of this report.

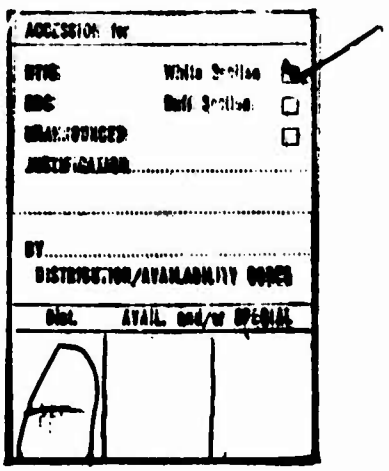

Technical Report Documentation Page

1. Report No.	2. Government Accession No.	3. Recipient's Catalog No.
FAA-RD-74-34-I		AD/A-000456

4. Title and Subtitle
PRESTRESSED CONCRETE PAVEMENTS; VOLUME I: DULLES TEST ROAD INSTRUMENTATION AND LOAD TESTS

5. Report Date
October 1974

6. Performing Organization Code

8. Performing Organization Report No.

7. Author(s)
Eugene C. Odom, Richard H. Ledbetter

9. Performing Organization Name and Address
U. S. Army Engineer Waterways Experiment Station
Soils and Pavements Laboratory
Vicksburg, Miss. 39180

10. Work Unit No. (TRAIS)

11. Contract or Grant No.
FA71WAI-218

12. Sponsoring Agency Name and Address
U.S. Department of Transportation
Federal Aviation Administration
Federal Highway Administration
Washington, D. C. 20591

13. Type of Report and Period Covered
Final report

14. Sponsoring Agency Code

15. Supplementary Notes

16. Abstract

This report describes the instrumentation of a prestressed concrete test road and the data obtained from a series of load tests conducted on the test road and presents an analysis of the data. The test road was constructed near Dulles International Airport, Washington, D. C., by the Federal Highway Administration. Bison strain sensors and U. S. Army Engineer Waterways Experiment Station and URS pressure cells were used to measure the strains, stresses, and deflections in the prestressed pavement, cement-treated base, and subgrade. Load tests were conducted using a truck to represent highway loads and a load cart with a simulated Boeing 747 aircraft gear to represent aircraft loads.

Design and construction procedures for prestressed concrete civil airport pavements are presented in Volume II of this report.

17. Key Words	18. Distribution Statement
Prestressed concrete pavements Instrumentation Load tests	Document is available to the public through the National Technical Information Service, Springfield, Va. 22151.

19. Security Classif. (of this report)	20. Security Classif. (of this page)	21. No. of Pages	22. Price
Unclassified	Unclassified	58	4.25

Form DOT F 1700.7 (8-72) Reproduction of completed page authorized

PREFACE

The study reported herein was jointly sponsored by the Federal Aviation Administration as part of Inter-Agency Agreement FA71WAI-218, "Development of Airport Pavement Criteria," and by the Federal Highway Administration under Order No. 1-102191, "Case Studies of Pavement Performance." The study was conducted during July 1971-March 1974.

The study was conducted under the general supervision of Mr. James P. Sale, Chief, Soils and Pavements Laboratory, of the U. S. Army Engineer Waterways Experiment Station (WES). This report was prepared by Messrs. Eugene C. Odom and Richard H. Ledbetter.

Directors of WES during the conduct of the investigation and the preparation of this report were BG E. D. Peixotto, CE, and COL G. H. Hilt, CE. Technical Director was Mr. F. R. Brown.

TABLE OF CONTENTS

CONVERSION FACTORS, U. S. CUSTOMARY TO METRIC (SI) UNITS OF MEASUREMENT

U. S. customary units of measurement used in this report can be converted to metric (SI) units as follows:

Multiply	By	To Obtain
inches	2.54	centimeters
feet	0.3048	meters
square inches	6.4516	square centimeters
miles per hour	1.609344	kilometers per hour
kips	4.448222	kilonewtons
pounds per square inch	0.6894757	newtons per square centimeter
pounds per cubic inch	0.0276799	kilograms per cubic centimeter

INTRODUCTION

BACKGROUND

The tests reported herein were sponsored by the Federal Aviation Administration (FAA) and the Federal Highway Administration (FHWA). The prestressed concrete highway pavement evaluated was a part of the airport road network serving the 1972 International Exposition (TRANSPO 72) located near Dulles International Airport, Washington, D. C. It was designed by the FHWA and constructed under its Research and Development Demonstration Projects Program with the objective of demonstrating that prestressed concrete pavement construction is practical and economically competitive with that of other types of pavements.

PURPOSE AND SCOPE

This report presents the data and an analysis resulting from a series of tests conducted on the prestressed concrete highway pavement. The tests consisted of measurements of stress and strain in the prestressed concrete pavement soil system structure under various loading conditions. Strain gages and pressure cells were installed by the U. S. Army Engineer Waterways Experiment Station (WES) in two separate prestressed concrete slabs and in the underlying subgrade to measure the pavement response under load. The tests were designed to provide data to assist in validating design criteria for airport pavements being developed by WES for the FAA. Tests were conducted using a truck to represent highway loads and a load cart equipped with one dual-tandem component of a Boeing 747 aircraft main landing gear to represent aircraft loadings.

Additional instrumentation was installed and tests performed by the FHWA. The instrumentation and results of these tests are described in Reference 1.

CONSTRUCTION OF TEST ROAD

A detailed description of the construction of the test road at Dulles is given in Reference 2. The test road (Figure 1) consisted of a 24-ft-wide,* 3200-ft-long, 6-in.-thick roadway. The six prestressed concrete slabs included in the roadway ranged in length from 400 to 760 ft. Each slab was prestressed to 200 psi at the slab ends by means of twelve 1/2-in.-diam, 7-wire, high-strength steel strands placed on 24-in. centers. These strands were located 1/2 in. below middepth of the slabs. After the concrete was placed, a tensile force of 29 kips (70 percent of ultimate strength) was applied on each strand.

The strands were stressed by hydraulic jacks bearing against 6-in. I-beams at the ends of each slab. These I-beams were part of the expansion joints between slabs and also helped to reinforce the pavement at the joints. To provide working space for the prestressing process, 8-ft gaps were left between each prestressed slab. After the prestressing, the gaps were filled with reinforced concrete.

The prestressed pavement was constructed over a 6-in.-thick, 28-ft-wide cement-treated crushed stone base. The cement content of the base was 4 percent by weight, and the crushed stone aggregate conformed to the Virginia Department of Highways gradation size No. 21A.[1] The gradation of the crushed stone aggregate is shown in the following tabulation:

Sieve Size	Percent by Weight Passing
2 in.	100 (min)
1 in.	95 ±5
3/8 in.	67 ±17
No. 10	38 ±12
No. 40	21 ±9
No. 200	10 ±5

The subgrade consisted of a clay classified A-6(12) according to the American Association of State Highway Officials (AASHO) Designation:

---

* A table of factors for converting U. S. customary units of measurement to metric (SI) units is presented on page 4.

M 145-66[3] (FAA E-7 soil group[4]) overlying clay shale. Compaction requirements for the A-6(12) material are not less than 95 percent of maximum dry density. The final grade included both cut and compacted fill sections with excavations into the clay shale in some of the cut sections.

INSTRUMENTATION

Instrumentation for the prestressed concrete sections consisted of strain sensors and pressure cells. These devices were installed at various depths within the pavement structure in order to measure strain and stress.

STRAIN SENSORS

The strain gages used, called strain sensors, were manufactured by Bison Instruments, Inc. The strain gage system, which is described in References 5 and 6, consisted of sensors and an external instrument package. The sensors are individual disk-shaped coils, and their principle of operation involves the mutual inductance coupling of any two coil sensors which can be placed in one of three alignments with respect to each other: lateral, parallel, or perpendicular. Only lateral and parallel alignments were used in these tests. Separation of the coils is sensed by measuring the electromagnetic coupling between the two sensors. The change in electromagnetic coupling is a nonlinear function of the relative movement of the coils; however, the change can be calibrated very accurately with resolution of spacing change better than 0.0001 in. The coils have no mechanical connection between them, and they can be operated at any spacing between one and four times the nominal coil diameter as long as there is no disturbance of the induced electromagnetic field, such as metal between or around the coils. Four-in.-diam coils were used in this study. Figure 2 shows two of the coils in a micrometer calibration mount.

The external instrument package to which the sensors are connected is a field-use instrument that contains all necessary driving, amplification, balancing, readout, and calibration controls and has a self-contained power supply. Changes in coil spacing can be determined by means of a bridge balance, meter deflection from zero, or voltage output on a recorder connected to the rear panel of the instrument package. The instrument package used for this study detected both static and dynamic strain. Response of the instrument was about 0.1 msec.

PRESSURE CELLS

Vertical pressures were measured by WES soil pressure cells (Figure 3a) and by a URS pressure cell (Figure 3b). The WES cell, which is described in References 7 and 8, is 6 in. in diameter and 1 in. thick overall. It is fabricated from stainless steel and consists of a circular faceplate, provided with a peripheral slot that forms a flexural joint, welded at its perimeter to a thicker baseplate. A thin cavity formed between the faceplate and baseplate is mercury filled so that pressure on the faceplate is averaged and transmitted by the liquid to an internal diaphragm. The diaphragm is formed by boring the baseplate blank from the rear to provide an integral thin section that will deflect linearly and consistently under loading. Affixed to the rear of this diaphragm is a full Wheatstone bridge circuit consisting of four electrical SR-4 strain gages hermetically sealed within the cell. The strain gages undergo resistance change proportional to strains in the diaphragm induced by applied pressure on the faceplate that is transmitted through the mercury. Temperature effects in the strain gages and resistance variations in the lead wires are practically eliminated by the full Wheatstone bridge. Temperature effects in the force-summing mercury chamber are minimized by the choice of materials. The cell measures the total pressure from both the solid and the liquid phases of the soil. Compression occurs normal to the two parallel faces of the cell, and the active pressure is averaged over the whole faceplate with the large area serving to smooth out local stress concentrations. Only the soil pressure component normal to the faceplate is effective in operating the cell. Calibration of the WES soil pressure cell is performed by correlating the electrical response of the cell, as measured by an SR-4 indicator, with the load that produces the cell response. For the study reported herein, the dead-load method was used to calibrate the pressure cells. Dead-load calibration is accomplished in a double-diaphragm pneumatically actuated calibrating chamber for applying uniform loads to the faceplate. Repeatability of the WES cell is approximately 5.6 percent, and accuracy is to within 10 percent of the indication.

The URS soil pressure cell developed by the URS Research Company for the FHWA is shown in Figure 3b. This cell was designed, constructed, and evaluated by the URS Research Company and is fully described in Reference 9. Both static and dynamic stresses can be measured by this gage. The URS pressure cell is 0.06 in. thick and 1.5 in. in diameter and consists of a sensing element of a piezoresistive semiconductor strain gage in a fluid cavity. Evaluation tests conducted by URS indicated that the cell has high sensitivity, flat frequency response from 100 to 0 kHz, and high repeatability.

INSTRUMENTATION LOCATION

A plan and cross section of the east and west slabs showing locations of the instrumentation are presented in Figures 4 and 5, respectively. The east slab was constructed mainly in a cut section in which the excavation was carried into the underlying clay shale, while the subgrade of the west slab consisted primarily of compacted fill. As shown in these figures, instrumentation was placed at three different sites (A, B, and C) within both 500-ft slabs. The two slabs are hereinafter referred to as the east and west "test sections."

Each of the six gage locations had four Bison coils aligned vertically at approximately the same depth. One coil was placed at the top of the cement-treated base, and the other three coils were placed at distances of 13, 23, and 29 in. below the pavement surface. This placement allowed measurement of the vertical movement between any two coils. In addition to the four vertically aligned coils, points A-3 and B-3 in both slabs had one pair of laterally aligned coils in the top of the pavement and one pair in the bottom of the pavement. These coils were aligned parallel to the pavement edge. Point A-3 also had two pairs of coils in a parallel alignment at an approximate depth of 18 in. that were used to measure horizontal strain in the subgrade. One pair was placed parallel to the pavement edge to measure longitudinal strain, while the other pair was perpendicular to the pavement edge to measure transverse strain. There were also three pressure cells placed in the top of the base to measure the interface pressure between the prestressed

concrete pavement and the base course.

At site C in both test sections, there were seven vertical stacks of Bison coils and one stack in each adjacent transition section. The purpose of the gages at site C was to measure any slab curl or slab movement under load. This study was the first in which Bison strain sensors have been used in an effort to measure any type of slab movement such as curling. It was felt that, although this use might be beyond the limits of the Bison strain sensors in their present stage of development, the effort might nevertheless prove worthwhile.

Each of the seven stacks at site C consisted of three Bison coils at about the same depth in all sixteen locations. One coil was placed in the top of the pavement, one coil was placed at the top of the base, and the other coil was placed 13 in. below the pavement surface.

Several aspects of instrumentation installation and location are shown in Figures 6-10. Figure 6 shows the removable forms used for installation of strain sensors in the slab, and Figure 7 shows a Bison strain sensor in a waterproof bag at a location on top of the base course. Figure 8 shows the strain gage pattern for the slab corner, and Figure 9 shows a strain sensor being checked ahead of the concrete finisher. Figure 10 shows instruments used for recording data.

LOADING CONDITIONS

For the load tests, two types of loadings were employed. The first series of tests used a three-axle truck (Figure 11) and is hereinafter referred to as the "truck tests." The truck was a semitrailer combination vehicle with single drive and trailer axles spaced 20 ft on center and equipped with dual-tire wheels. The second series of tests used the load cart shown in Figure 12, in which one dual-tandem component of a Boeing 747 aircraft main landing gear was placed. These tests are hereinafter referred to as the "load cart tests." The load cart consisted of an outer support frame and a load compartment into which the gear was placed. Lead weights were placed in the load compartment to provide the desired test load.

TRUCK TESTS

During the period 24-28 January 1972, truck tests were conducted using a single-axle, dual-wheel load on the two instrumented slabs. The rear axle of the truck, with loads of approximately 19.5 and 33.2 kips, was used for the tests. The tires were 12.00x24 truck tires inflated to an average tire pressure of 96 psi and an average contact area of 80 sq in. for the 19.5-kip load and 108 sq in. for the 33.2-kip load. Crushed stone available at the site was used to load the vehicle.

The axle arrangements and tire spacings for the truck are shown in Figure 13a. Figure 14a shows the rear axle placement for the two primary loading positions used in the truck tests. Loading position 1 consisted of centering either the left or right set of dual tires over a loading point. Loading position 2 consisted of placing the midpoint of the rear axle over a loading point. A typical truck test on a loading point is shown in Figure 15. Both static and moving tests were conducted; the moving tests involving speeds up to 45 mph. Moving tests were conducted with the 19.5-kip load over the gages in the east test section and the 33.2-kip load over the gages in the west test section.

Due to insufficient time and bad weather conditions, the points at site C of both slabs were not individually loaded. However, a few

selected loading points were chosen, and all of the gages at site C were read while the truck was placed over these points. For the east test section, loading points C-3 and C-13 were loaded with the truck placed in loading position 1. Four loading points were selected for the west test section. The rear axle midpoint (position 2) was placed 6 ft from the north pavement edge at distances of 100, 40, and 20 in. from the joint and also directly over the joint. These loading points are shown in Figure 16 and are labelled points 3, 4, 5, and 6, respectively.

LOAD CART TESTS

The second series of tests was conducted from 21-30 October 1972. Loadings were applied using a simulated aircraft landing gear positioned in the load cart. The tires and tire spacings were identical with those of a dual-tandem main gear of the Boeing 747, as shown in Figure 13b. Lead weights were used to obtain the two test loads of 60 and 100 kips. With the 60-kip load, the tire inflation pressure was 45 psi, while with the 100-kip load the inflation pressure was 85 psi. The tire contact area was maintained constant at 285 sq in. for both loads. The two main loading positions for these tests are shown in Figure 14b. Loading position 1 consisted of placing one of the four tires over a loading point, while loading position 2 consisted of centering the gear arrangement over a loading point.

PAVEMENT EVALUATION

An evaluation of the prestressed concrete pavement showed that the test loads were conservative compared to the static failure load capacity, especially for the truck. The pavement was evaluated using the methodology described in Volume II of this report.[10]

For this evaluation, the following assumptions were made:

a. Concrete modulus of elasticity of 5×10^6 psi.

b. Poisson's ratio of concrete of 0.20 percent.

c. Concrete flexural strength of 650 psi.

d. Subgrade restraint of 156 psi.

e. Temperature warping stress of 90 psi.

f. Moduli of subgrade reaction of 300 pci and 500 pci for the west and east test sections, respectively.

The moduli of subgrade reaction were based on theoretical considerations discussed in the analysis section of this report.

Using the effective prestress equation from Volume II,[10] the single-wheel static failure loads were computed for each test section and for each vehicle. The single-wheel static failure loads for a tire contact area of 82 sq in. (approximately equal to the tire contact area of the rear dual wheels of a truck) were as follows:

a. West test section load of 58.927 kips.

b. East test section load of 62.808 kips.

These failure loads would correspond approximately to a single-wheel truck axle load of 120 kips, an even greater single-axle dual-wheel load, and a slightly smaller dual-axle load. By the use of any fatigue criterion, the prestressed highway section should carry a large number of such loadings. It is evident therefore that the vehicular test load applied was light, and small strains or deflections such as those measured should have occurred.

Computed single-wheel static failure loads for the dual-tandem aircraft gear were as follows:

a. West test section load of 73.659 kips.

b. East test section load of 76.295 kips.

Using the single- and multiple-wheel gear relations in Volume II results in dual-tandem failure loads of 159.103 and 164.034 kips, respectively, for the west and east test sections. The pavement evaluation therefore indicates that stresses and strains in the pavement soil system structure should also be small for the aircraft landings.

TEST DATA

Data obtained from the load tests are presented in Tables 1-11. Included in these tables are the strain and pressure data obtained using the truck and load cart. Strain measurements represent the elastic deformation that occurs within the pavement structure and were determined by subtracting the loaded gage spacing from the unloaded spacing. In reducing the data, correction was made for the effects of metal of the truck and load cart influencing the electromagnetic coupling between sensors. This correction factor is constant for each vehicle and for specific distances and gage spacings. The constant is easily determined with a pair of gages and only needs to be subtracted from the in-place measurements. Metal effects from the steel in the concrete slabs shift the calibration curves by a constant and do not significantly change the slope; therefore, no correction was needed for this effect.

Data in Tables 1-9 include the load, gage location, gage depth, gage spacing, change in gage spacing, and the resulting strain. Strain was recorded for static loads and for moving truck loads. With the equipment used in the static load tests, the movement of the pavement structure between any two Bison coils was manually read with a field-use Bison indicator and recorded to an accuracy of 0.001 in. Thus, when the change in gage spacing in the data tables is listed as <0.001, the movement was too small to be accurately detected. This type of reading does not indicate that the gages had failed. With the moving load tests the movements were automatically recorded with a strip chart recorder and scaled to an accuracy of 0.0001 in. The gage data for warping and curling movements at location C are not presented in these tables because these movements were all less than the accuracy of the measurement system.

Pressure cell readings were obtained and are shown in Tables 10 and 11. These tables show the stresses resulting from various positions of the loading vehicles.

Immediately after construction, an examination of the gages showed that 10 of the Bison coils were not functioning. Five of these

coils were in the west test section. One of these was the coil in the top of the pavement at point C-6, another was one of the lateral pair in the bottom of the pavement at point A-3, and one was in the bottom of the pavement at point C-5. The other two were at point C-4 in the bottom of the pavement and at a depth of 13 in. The other five nonworking coils were in the east test section. Two of these were in the bottom of the pavement at points A-2 and A-3, and two were in the top of the pavement at points C-2 and C-9. The fifth coil was one of the lateral pair in the top of the pavement at point C-6. When the load cart tests began, one other coil was discovered to be not working. This coil was one of the lateral pair in the top of the pavement at point A-3 in the west test section. Also, for the load cart tests, the WES pressure cell in the west test section did not read as properly as it did for the truck tests, and the URS pressure cell in the east test section also did not read properly. The malfunctions of these gages could have been due to damage to the leads or displacement of the gages during construction. Due to these nonworking strain sensors, there are gaps in the strain data in the tables.

DATA ANALYSIS

In order to analyze the instrumentation data, theoretical stresses and deflections were calculated for comparison with measured values. Theoretical total deflections were determined using influence charts developed by Pickett and Ray,[11] which assume the subgrade to be a dense liquid. These deflections, based upon the edge and interior loading conditions, were calculated for both loading positions of the 19.5- and 33.2-kip axle loads in the truck tests and the 60- and 100-kip gear loads in the load cart tests.

To determine the pavement and subgrade stresses and the approximate distribution of the subgrade displacements, a computer program[12] developed by the Koninklijke/Shell-Laboratorium, Amsterdam, was used. This program was devised as a general-purpose program for computing horizontal and vertical stresses, strains, and displacements in elastic multilayered systems subjected to one or more uniform loads. Values of the modulus of elasticity E and Poisson's ratio ν were assumed for each layer in the system.

In analyzing the data, one desired comparison was of the measured displacements with theoretical deflections. In calculating theoretical deflections, it was necessary to assume different values for the modulus of subgrade reaction k in the east and west test sections. A difference in subgrade strength was expected because the west test section was constructed on compacted fill while the subgrade of the east test section was a clay shale. Thus, a k value of 300 pci was assumed for the west test section, and a k of 500 pci was assumed for the east test section.

VERTICAL STRAIN; STATIC LOAD TESTS

SUBGRADE

The subgrade performance under the prestressed concrete pavement is indicated by the subgrade strains and deflections. To analyze this performance, the average subgrade strains and partial displacements were determined for the west test section (Table 12) and for the east test

section (Table 13). An initial examination of the data shows that, for both vehicle load positions, measured strain in the 13- to 23-in. depth or top increment of the subgrade was larger than the measured strain in the 23- to 29-in. depth or bottom increment. This trend is to be expected since the vertical stress and strain should decrease with depth under all load positions if no soft soil layers exist.

Some of the test data were plotted showing accumulated measured vertical elastic displacement with depth below the pavement surface. To permit plotting of the data, the Bison coils at the 29-in. depth had to be assumed as a zero reference since no measurements were made below that depth. However, this assumption does not mean that no displacement occurred below the 29-in. depth. The accumulated elastic displacement for one of the 12 interior load points is shown in Figure 17, which is a plot of the data from point B-3 in the west test section. Average accumulated measured elastic displacements for the six interior load points for the west test section are shown in Figure 18, while Figure 19 shows a similar plot for the east test section. The data in Figures 17a, 18a, and 19a were obtained with the truck and load cart in loading position 1, while the data in Figures 17b, 18b, and 19b were obtained with the truck and load cart in position 2.

A comparison of the measured subgrade displacements (elastic change in gage spacing) under the east and west slabs was made by ratioing the west subgrade displacement to the east subgrade displacement. These ratios are shown in Table 12. They were approximately the same for the four load cart loadings, with the displacements in the west test section averaging about 2.7 times the displacements in the east test section. An accurate comparison is difficult to make for the truck load displacements in the two test sections because the displacements in the east test section were very small.

Theoretical total deflections determined using the Pickett and Ray influence charts are shown in Tables 14 and 15 for the west and east test sections, respectively. Since the theoretical values were to be compared with the measured values, reasonable theoretical values at the load points were desired. To compare edge deflections with the measured

values would not be satisfactory since there were no measurements made at the pavement edge. In addition, the theoretical interior deflections were not considered to be reasonable values for comparison because the measurement locations were too close to either the edge or the center-line longitudinal joint. The theoretical interior deflections were then compared to the theoretical edge deflections considering one tire of the Boeing 747 gear and the center of the dual truck tires as being over the load point. The interior deflections were found to be 40 percent of the edge deflections. For a vehicle, a reasonable theoretical value was then assumed to lie between the edge and interior deflections. Therefore, a value halfway between these values was assumed that was equal to 175 percent of the interior deflection or 70 percent of the edge deflection. These are the theoretical values shown in the tables. Theoretical interior deflections were also calculated considering the center of the gear and the midpoint of the axle as being over the loading point (load position 2). These deflections were approximately the same as the theoretical interior deflections for loading position 1. Therefore, the theoretical deflections shown in Tables 14 and 15 are the same for both vehicle loading positions.

Tables 14 and 15 also present a comparison of the measured displacements with the theoretical deflections as determined above. The displacements for the 13- to 23-in. and the 23- to 29-in. depths were combined for comparison with the theoretical deflections. This comparison indicates that the measured displacements for the west test section ranged from 31 to 46 percent of the theoretical total deflections and from 13 t 23 percent for the east test section. For the east test section, the ratio of the measured displacements to the theoretical deflections generally remained constant for both the truck and the gear loadings. This trend indicates that the subgrade of the east test section was responding linearly within the range of loads used in the tests. For the west test section, the percentage of the theoretical total deflections appeared to increase with an increase in applied load, thus indicating that the subgrade response in the west test section may have been nonlinear. However, since the measured displacements for the truck

loads on the east test section were near the lower limit of the range of accuracy of the measuring instruments, no valid conclusions can be drawn.

Table 16 presents a comparison of the measured displacements in the subgrade with the theoretical displacements as computed by the Shell multilayered computer program. For the data analysis, the modulus of elasticity of the 6-in. prestressed concrete pavement was assumed to be 5×10^6 psi and Poisson's ratio was assumed as 0.20. The 6-in. cement-treated base was assumed to have a modulus of elasticity of 5×10^4 psi and a Poisson's ratio of 0.30. This modulus, which was assumed based upon repetitive load test results that have been conducted on similar materials, seems low when compared with a modulus determined from laboratory flexural tests. However, field modulus values determined from beams cut from cement-treated bases have shown modulus values much lower than laboratory values. Thus, the 5×10^4 psi value was considered representative of the performance to be expected.

As with the influence charts, two values of subgrade strength were assumed for the two test sections. The underlying subgrade of the west test section was assumed to have a modulus of elasticity of 3×10^3 psi and a Poisson's ratio of 0.40. The modulus of elasticity of the east test section subgrade was assumed to be 15×10^3 psi, while Poisson's ratio was assumed to be 0.40.

As stated previously, an additional stronger layer of subgrade was added to the computer program for both the west and the east test sections to represent naturally occurring conditions. This layer was placed at a depth of 60 in. below the top of the pavement (48 in. below the bottom of the cement-treated base) and had a modulus of elasticity of 5×10^4 psi and a Poisson's ratio of 0.30. The measured displacements in both the east and the west test sections agreed reasonably well with the theoretical displacements determined with the computer program. One exception was under the 100-kip gear load in the east and west test sections where the measured displacements were larger than the theoretical displacements. A possible reason for this difference is that the subgrade was beyond its linear behavior range under this load.

CEMENT-TREATED BASE AND PRESTRESSED CONCRETE SURFACE

The measured vertical displacements and strains are shown in Tables 1, 2, 6, and 7 for the cement-treated base at sites A and B. The layer listed for the 6- to 13-in. depth included the cement-treated base and about 1 in. of the subgrade. The movement in this layer was too small to be measured for any of the test loadings, thus indicating non-compressibility of the stabilized layer. The instrumentation at site C of both test sections was placed to measure the slab curl or other slab movements under an applied load. There were no movements large enough to be detected; therefore, none of the readings from the gages at site C are listed in the tables.

HORIZONTAL STRAIN; STATIC LOAD TESTS

Table 17 shows theoretical horizontal stresses and strains calculated for the prestressed concrete pavement using the Shell multi-layered computer program. The measured strains are shown in Tables 3 and 4 for the truck tests and in Tables 8 and 9 for the load cart tests. The gages listed in the tables at a depth of 0 in. were used to measure the horizontal strain in the top of the pavement, while the gages at 6 in. were used to measure the horizontal strain in the bottom of the pavement. The only loading condition for which there was any measurable strain in the pavement was the 33.2-kip axle load of the truck tests in the west test section at loading position 1. As shown in Table 3 for points B-3 and C-6, the measured strains at the top and bottom of the pavement were -1 and $+2 \times 10^{-4}$ in./in., respectively. These measured strains compare favorably with the theoretical strains of -1 and $+1 \times 10^{-4}$ in./in. for the same loading conditions. For all other loading conditions, no strains could be measured. Table 18 gives a comparison of the measured horizontal strain in the subgrade at a depth of 18 in. with the theoretical horizontal strain at the same depth as computed by the Shell program. The measured horizontal strains were at point A-3 in the west test section and at point B-3 in the east test section. The spacing and change in spacing of these gages are shown in Tables 3 and 4 for the truck tests and in Tables 8 and 9 for the load cart tests. Some

of the measured strains agreed fairly well with the theoretical strains, but in general the measured values were quite different from the theoretical values.

VERTICAL PRESSURES; STATIC LOAD TESTS

A comparison of the measured and theoretical vertical stresses at the bottom of the pavement slab is shown in Table 19. The stresses measured in the east and west test sections for the two truck loads were about the same as the theoretical stresses computed by the Shell program. In the east test section, the measured stresses for the two load cart loads were much less than the theoretical values. Compared to the truck tests, the measured stresses for the load cart tests in the east test section appeared to be too low. Since the load cart tests were conducted 9 months after the truck tests, there could be several reasons for the measured values being lower. The foundation strength may have deteriorated due to saturation of the subgrade, or there may have been an increase in the prestress or concrete strength.

MOVING LOAD TESTS

Vertical and horizontal elastic strain data for the moving truck tests are shown in Table 5. The vertical strain in the subgrade remained relatively constant for all three test speeds, and no horizontal pavement strains could be measured. The measured vertical strain did agree well with the theoretical static vertical strain. Therefore, based on limited testing, it appears that the vertical elastic strain in the subgrade may remain constant within the range of speeds used in these tests.

The pressure cell data for the moving truck tests are given in Table 10. Only the output of the WES pressure cells was recorded during the speed tests. From the limited test data, it appears that the vertical pressure under the pavement may also remain constant within the range of test speeds. This conclusion agrees with the results for subgrade vertical strain under moving loads.

CONCLUSIONS

Based upon the results of these tests, the following conclusions are believed warranted:

a. Strains measured in the subgrade under static and moving loads agreed reasonably well with calculated theoretical values.

b. The field readout equipment and procedure were not accurate enough to detect the small horizontal strains in the slabs or small vertical strains in the stabilized layers.

c. The vertical stress measurements made under static and moving truck loads also agreed reasonably well with calculated theoretical stresses. However, vertical stresses measured under the load cart did not compare favorably with the theoretical stresses. The pressure cell response to the load cart appeared to be in error when compared with that of the truck loading.

d. The small strains and deflections measured in these tests indicate that the roadway should have a long service life.

TABLE 1.--VERTICAL STRAIN DATA, STATIC TRUCK TESTS
WEST SECTION, SITES A AND B

Load lb	Gage Location	Gage Depth in.	Gage Spacing in.	Change in Spacing, in.		Strain, 10^{-4} in./in.	
				Loading Position 1	Loading Position 2	Loading Position 1	Loading Position 2
19,500	A-1	6-13	8.87	<0.001		<1	
		13-23	10.09	<0.001		<1	
		23-29	6.15	<0.001		<1	
	A-2	6-13	7.52	<0.001	<0.001	<1	<1
		13-23	10.14	0.010	0.004	10	4
		23-29	6.05	<0.001	<0.001	<1	<1
	A-3	6-13	8.35	<0.001	<0.001	<1	<1
		13-23	10.19	0.011	0.008	11	8
		23-29	6.09	<0.001	<0.001	<1	<1
33,200	A-1	6-13	8.87	<0.001		<1	
		13-23	10.09	0.012		12	
		23-29	6.15	0.004		7	
	A-2	6-13	7.53	<0.001	<0.001	<1	<1
		13-23	10.14	0.009	0.009	9	9
		23-29	6.05	0.001	0.002	2	3
	A-3	6-13	8.35	<0.001	<0.001	<1	<1
		13-23	10.18	0.006	0.007	6	7
		23-29	6.09	0.002	0.001	3	2
19,500	B-1	6-13	7.86	<0.001		<1	
		13-23	10.04	<0.001		<1	
		23-29	6.45	<0.001		<1	
	B-2	6-13	8.42	<0.001	<0.001	<1	<1
		13-23	10.07	0.003	<0.001	3	<1
		23-29	6.37	0.001	0.001	2	2
	B-3	6-13	8.02	<0.001	<0.001	<1	<1
		13-23	10.19	0.001	0.002	1	2
		23-29	6.03	0.002	0.001	3	2
33,200	B-1	6-13	7.86	<0.001		<1	
		13-23	10.04	0.002		2	
		23-29	6.45	0.005		8	
	B-2	6-13	8.42	<0.001	<0.001	<1	<1
		13-23	10.07	0.004	0.004	4	4
		23-29	6.37	0.001	<0.001	2	<1
	B-3	6-13	8.02	<0.001	<0.001	<1	<1
		13-23	10.19	0.005	0.004	5	4
		23-29	6.03	0.003	0.002	5	3

TABLE 2.--VERTICAL STRAIN DATA, STATIC TRUCK TESTS
EAST SECTION, SITES A AND B

Load lb	Gage Location	Gage Depth in.	Gage Spacing in.	Change in Spacing, in.		Strain, 10^{-4} in./in.	
				Loading Position 1	Loading Position 2	Loading Position 1	Loading Position
19,500	A-1	6-13	10.19	< 0.001		<1	
		13-23	9.74	< 0.001		<1	
		23-29	6.27	< 0.001		<1	
	A-2	6-13	--				
		13-23	10.06	< 0.001		<1	
		23-29	5.74	< 0.001		<1	
	A-3	6-13	--				
		13-23	9.91	< 0.001		<1	
		23-29	6.24	< 0.001		<1	
33,200	A-1	6-13	10.19	< 0.001		<1	
		13-23	9.75	< 0.001		<1	
		23-29	6.27	< 0.001		<1	
	A-2	6-13	--				
		13-23	10.06	< 0.001	<0.001	<1	<1
		23-29	5.74	0.002	<0.001	3	<1
	A-3	6-13	--				
		13-23	9.91	< 0.001	<0.001	<1	<1
		23-29	6.24	0.002	<0.001	2	<1
19,500	B-1	6-13	12.05	< 0.001		<1	
		13-23	9.66	< 0.001		<1	
		23-29	6.27	< 0.001		<1	
	B-2	6-13	10.57	< 0.001		<1	
		13-23	9.68	< 0.001		<1	
		23-29	6.29	< 0.001		<1	
	B-3	6-13	10.57	< 0.001		<1	
		13-23	10.10	< 0.001		<1	
		23-29	5.89	< 0.001		<1	
33,200	B-1	6-13	12.04	< 0.001		<1	
		13-23	9.65	< 0.001		<1	
		23-29	6.27	0.002		3	
	B-2	6-13	10.57	< 0.001	<0.001	<1	<1
		13-23	9.68	< 0.001	<0.001	<1	<1
		23-29	6.29	< 0.001	<0.001	<1	<1
	B-3	6-13	10.56	< 0.001	<0.001	<1	<1
		13-23	10.10	0.001	<0.001	1	<1
		23-29	5.89	0.001	<0.001	2	<1

TABLE 3.--HORIZONTAL STRAIN DATA, STATIC TRUCK TESTS, WEST SECTION

Load lb	Gage Location	Gage Depth in.	Gage Spacing in.	Change in Spacing, in.			Strain, 10^{-4} in./in.		
				Loading Position 1	Loading Position 2	Midpoint of Axle Over Pavement Center Line	Loading Position 1	Loading Position 2	Midpoint of Axle Over Pavement Center Line
19,500	A-3 parallel	18	13.815	+0.008	+0.006	-0.009	+6	+4	-7
	A-3 perpendicular	18	14.105	+0.010	<0.001	<0.001	+7	<1	<1
	A-3	0	7.070	<0.001	<0.001	<0.001	<1	<1	<1
		6	--						
	B-3	0	7.43	<0.001	<0.001	<0.001	<1	<1	<1
		6	5.46	<0.001	<0.001	<0.001	<1	<1	<1
	C-6	0	7.16	<0.001	<0.001		<1	<1	
		6	5.19	<0.001	<0.001		<1	<1	
33,200	A-3 parallel	18	13.815	-0.001	+0.001	+0.001	-1	+1	+1
	A-3 perpendicular	18	14.105	-0.002	+0.003	<0.001	-1	+2	<1
	A-3	0	7.07	<0.001	<0.001	<0.001	<1	<1	<1
		6	--						
	B-3	0	7.43	-0.001	<0.001	<0.001	-1	<1	<1
		6	5.46	+0.001	<0.001	<0.001	+2	<1	<1
	C-6	0	7.16	-0.001	<0.001		-1	<1	
		6	5.19	+0.001	<0.001		+2	<1	

Note: + denotes tension; - denotes compression.

TABLE 4.--HORIZONTAL STRAIN DATA, STATIC TRUCK TESTS, EAST SECTION

Load lb	Gage Location	Gage Depth in.	Gage Spacing in.	Change in Spacing, in.			Strain, 10^{-4} in./in.		
				Loading Position 1	Loading Position 2	Midpoint of Axle Over Pavement Center Line	Loading Position 1	Loading Position 2	Midpoint of Axle Over Pavement Center Line
19,500	B-3 parallel	18	15.332	+0.006			+4		
	B-3 perpendicular	18	13.307	+0.006			+5		
	B-3	0	7.95	<0.001			<1		
		6	5.64	<0.001			<1		
	A-3	0	7.06	<0.001			<1		
		6	5.76	<0.001			<1		
	C-6	0	--						
		6	5.74	<0.001			<1		
33,200	B-3 parallel	18	15.332	-0.004	-0.003	<0.001	-3	-2	<1
	B-3 perpendicular	18	13.307	+0.004	+0.001	<0.001	+3	+1	<1
	B-3	0	7.95	<0.001	--	<0.001	<1		<1
		6	5.64	<0.001	--	<0.001	<1		<1
	A-3	0	7.06	<0.001	<0.001	<0.001	<1	<1	<1
		6	5.76	<0.001	<0.001	<0.001	<1	<1	<1
	C-6	0	--						
		6	5.74	<0.001	<0.001		<1	<1	

Note: + denotes tension; - denotes compression.

TABLE 5.--VERTICAL AND HORIZONTAL STRAIN DATA
MOVING TRUCK TESTS

Load lb	Gage Location	Gage Depth in.	Gage Spacing in.	Change in Spacing, in.			Strain, 10^{-4} in./in.		
				10 mph	25 mph	40 mph	10 mph	25 mph	40 mph
33,200	West Section Vertical B-3	13-23	10.19	0.0035	0.0030	0.0030	3.4	2.9	2.9
33,200	West Section Horizontal B-3	Top Pavement	7.43	<0.0001	<0.0001	<0.0001	<0.1	<0.1	<0.1
19,500	East Section Horizontal B-3	Top Pavement	7.95	<0.0001	<0.0001		<0.1	<0.1	

TABLE 6.--VERTICAL STRAIN DATA, STATIC LOAD CART TESTS
WEST SECTION

Load lb	Gage Location	Gage Depth in.	Gage Spacing in.	Change in Spacing, in.		Strain, 10^{-4} in./in.	
				Loading Position 1	Loading Position 2	Loading Position 1	Loading Position 2
60,000	A-1	6-13	8.87	<0.001		<1	
		13-23	10.09	0.004		4	
		23-29	6.15	0.003		5	
	A-2	6-13	7.52	<0.001	<0.001	<1	<1
		13-23	10.14	0.008	0.008	8	8
		23-29	6.05	0.005	0.005	8	8
	A-3	6-13	8.35	<0.001	<0.001	<1	<1
		13-23	10.19	0.008	0.008	8	8
		23-29	6.09	<0.001	<0.001	<1	<1
100,000	A-1	6-13	8.87	<0.001		<1	
		13-23	10.09	0.012		12	
		23-29	6.15	0.008		13	
	A-2	6-13	7.52	<0.001	<0.001	<1	<1
		13-23	10.14	0.017	0.017	17	17
		23-29	6.05	0.006	0.006	10	10
	A-3	6-15	8.35	<0.001	<0.001	<1	<1
		13-23	10.19	0.012	0.012	12	12
		23-29	6.09	0.003	0.004	5	7
60,000	B-1	6-13	7.86	<0.001		<1	
		13-23	10.04	0.010		10	
		23-29	6.45	0.001		2	
	B-2	6-13	8.42	<0.001	<0.001	<1	<1
		13-23	10.07	0.011	0.008	11	8
		23-29	6.37	0.005	0.002	8	3
	B-3	6-13	8.02	<0.001	<0.001	<1	<1
		13-23	10.19	0.008	0.008	8	8
		23-29	6.03	0.006	0.003	10	5
100,000	B-1	6-13	7.86	<0.001		<1	
		13-23	10.04	0.021		21	
		23-29	6.45	0.005		8	
	B-2	6-13	8.42	<0.001	<0.001	<1	<1
		13-23	10.07	0.021	0.017	21	17
		23-29	6.37	0.008	0.004	13	6
	B-3	6-13	8.02	<0.001	<0.001	<1	<1
		13-23	10.19	0.017	0.017	17	17
		23-29	6.03	0.008	0.008	13	13

TABLE 7.--VERTICAL STRAIN DATA, STATIC LOAD CART TESTS
EAST SECTION

Load lb	Gage Location	Gage Depth in.	Gage Spacing in.	Change in Spacing, in.		Strain, 10^{-4} in./in.	
				Loading Position 1	Loading Position 2	Loading Position 1	Loading Position 2
60,000	A-1	6-13	10.19	<0.001		<1	
		13-23	9.74	0.002		2	
		23-29	6.27	<0.001		<1	
	A-2	6-13	--				
		13-23	10.06	0.003	0.003	3	3
		23-29	5.74	0.002	0.002	3	3
	A-3	6-13	--				
		13-23	9.91	<0.001	<0.001	<1	<1
		23-29	6.24	0.001	0.001	2	2
100,000	A-1	6-13	10.19	<0.001		<1	
		13-23	9.74	0.007		7	
		23-29	6.27	0.001		2	
	A-2	6-13	--				
		13-23	10.06	0.007	0.007	7	7
		23-29	5.74	0.005	0.005	9	9
	A-3	6-13	--				
		13-23	9.91	0.002	0.002	2	2
		23-29	6.24	0.002	0.002	3	3
60,000	B-1	6-13	12.05	<0.001		<1	
		13-23	9.66	0.003		3	
		23-29	6.27	0.002		3	
	B-2	6-13	10.57	<0.001	<0.001	<1	<1
		13-23	9.68	0.003	0.003	3	3
		23-29	6.29	0.002	<0.001	3	0
	B-3	6-13	10.57	<0.001	<0.001	<1	<1
		13-23	10.10	0.002	0.002	2	2
		23=29	5.89	<0.001	<0.001	<1	<1
100,000	B-1	6-13	12.05	<0.001		<1	
		13-23	9.66	0.007		7	
		23-29	6.27	0.003		5	
	B-2	6-13	10.57	<0.001	<0.001	<1	<1
		13-23	9.68	0.007	0.007	7	7
		23-29	6.29	0.003	0.003	5	5
	B-3	6-13	10.57	<0.001	<0.001	<1	<1
		13-23	10.10	0.004	0.004	4	4
		23-29	5.89	0.001	0.001	2	2

TABLE 8.--HORIZONTAL STRAIN DATA, STATIC LOAD CART TESTS
WEST SECTION

Load kips	Gage Location	Gage Depth in.	Gage Spacing in.	Change in Spacing, in. Loading Position 1	Change in Spacing, in. Loading Position 2	Strain, 10^{-4} in./in. Loading Position 1	Strain, 10^{-4} in./in. Loading Position 2
60	A-3 parallel	18	13.815	-0.001	-0.002	-1	-1
	A-3 perpendicular	18	14.105	+0.002	+0.002	+1	+1
	A-3	C	--				
		6	--				
	B-3	0	7.43	<0.001	<0.001	<1	<1
		6	5.46	<0.001	<0.001	<1	<1
	C-6	0	7.16	<0.001	<0.001	<1	<1
		6	5.19	<0.001	<0.001	<1	<1
100	A-3 parallel	18	13.815	+0.008	-0.003	+5	-2
	A-3 perpendicular	18	14.105	-0.003	+0.003	-2	+2
	A-3	0	--				
		6	--				
	B-3	0	7.43	<0.001	<0.001	<1	<1
		6	5.46	<0.001	<0.001	<1	<1
	C-6	0	7.16	< 0.001	< 0.001	< 1	< 1
		6	5.19	< 0.001	< 0.001	< 1	< 1

Note: + denotes tension, - denotes compression.

TABLE 9.--HORIZONTAL STRAIN DATA, STATIC LOAD CART TESTS
EAST SECTION

Load kips	Gage Location	Gage Depth in.	Gage Spacing in.	Change in Spacing, in.		Strain, 10^{-4} in./in.	
				Loading Position 1	Loading Position 2	Loading Position 1	Loading Position 2
60	B-3 parallel	18	15.332	<0.001	+0.004	<1	+3
	B-3 perpendicular	18	13.307	+0.004	+0.004	+3	+3
	B-3	0	7.95	<0.001	<0.001	<1	<1
		6	5.64	<0.001	<0.001	<1	<1
	A-3	0	7.06	<0.001	<0.001	<1	<1
		6	5.76	<0.001	<0.001	<1	<1
	C-6	0	--				
		6	5.74	<0.001	<0.001	<1	<1
100	B-3 parallel	18	15.332	+0.002	+0.004	+1	+3
	B-3 perpendicular	18	13.307	+0.004	+0.004	+3	+3
	B-3	0	7.95	<0.001	<0.001	<1	<1
		6	5.64	<0.001	<0.001	<1	<1
	A-3	0	7.06	<0.001	<0.001	<1	<1
		6	5.76	<0.001	<0.001	<1	<1
	C-6	0	--				
		6	5.74	<0.001	<0.001	<1	<1

Note: + denotes tension; - denotes compression.

TABLE 10.--PRESSURE CELL DATA
STATIC AND MOVING TRUCK TESTS

Load, kips	Position of Rear Dual Tires	URS Pressure Static psi	WES Pressure, psi			
			Static	10 mph	25 mph	40 mph
East Section						
19.5	Over Cell	3	3	3	3	
19.5	2 ft Past Cell	2	1			
33.2	Over Cell	5	5			
West Section						
19.5	Over Cell		2			
33.2	Over Cell (Average of 2 runs)		4	4	4	5

TABLE 11.--PRESSURE CELL DATA, STATIC
LOAD CART TESTS, EAST SECTION

Position of Rear Tire	Pressure, psi	
	60-kip Load	100-kip Load
Over Cell	2	4
4 ft Past Cell	<1	1
8 ft Past Cell	<1	<1
Position of Load Cart Center		
Over Cell	1	4
4 ft Past Cell	1	3
8 ft Past Cell	<1	<1

TABLE 12.--AVERAGE VERTICAL STRAIN DATA
STATIC LOAD TESTS, WEST SECTION

Load	Average Strain, 10^{-4} in./in., at Cited Depth		Average Displacement, in., at Cited Depth			Percent of East Section Movement at 13- to 29-in. Depth
	13-23 in.	23-29 in.	13-23 in.	23-29 in.	13-29 in.	
19.5-kip Truck Axle Loading Position 1	4	2	0.004	0.001	0.005	
33.2-kip Truck Axle Loading Position 1	6	4	0.006	0.002	0.008	400
60-kip Load Cart Loading Position 1	8	5	0.008	0.003	0.011	275
100-kip Load Cart Loading Position 1	17	10	0.017	0.006	0.023	288
19.5-kip Truck Axle Loading Position 2	3	2	0.003	0.001	0.004	
33.2-kip Truck Axle Loading Position 2	6	3	0.006	0.002	0.008	
60-kip Load Cart Loading Position 2	8	4	0.008	0.002	0.010	250
100-kip Load Cart Loading Position 2	16	9	0.016	0.005	0.021	263

TABLE 13.--AVERAGE VERTICAL STRAIN DATA
STATIC LOAD TESTS, EAST SECTION

Load	Average Strain, 10^{-4} in./in., at Cited Depth		Average Displacement, in., at Cited Depth			Percent of West Section Movement at 13- to 29-in. Depth
	13-23 in.	23-29 in.	13-23 in.	23-29 in.	13-29 in.	
19.5-kip Truck Axle Loading Position 1	<1	<1	<0.001	<0.001	<0.001	
33.2-kip Truck Axle Loading Position 1	1	2	0.001	0.001	0.002	25
60-kip Load Cart Loading Position 1	3	2	0.003	0.001	0.004	36
100-kip Load Cart Loading Position 1	6	4	0.006	0.002	0.008	35
19.5-kip Truck Axle Loading Position 2	No tests run					
33.2-kip Truck Axle Loading Position 2	<1	<1	<0.001	<0.001	<0.001	
60-kip Load Cart Loading Position 2	3	1	0.003	0.001	0.004	40
100-kip Load Cart Loading Position 2	5	5	0.005	0.003	0.008	38

TABLE 14.--COMPARISON OF MEASURED SUBGRADE MOVEMENT WITH THEORETICAL DEFLECTION, STATIC LOAD TESTS WEST SECTION

Load	Theoretical Total Deflection in. k = 300	Average Measured Displacement in.			Percent of Theoretical Total Deflection		
		13-23 in.	23-29 in.	13-29 in.	13-23 in.	23-29 in.	13-29 in.
19.5-kip Truck Axle Loading Position 1	0.013	0.004	0.001	0.005	31	8	38
33.2-kip Truck Axle Loading Position 1	0.022	0.006	0.002	0.008	27	9	36
60-kip Load Cart Loading Position 1	0.029	0.008	0.003	0.011	28	10	38
100-kip Load Cart Loading Position 1	0.050	0.017	0.006	0.023	34	12	46
19.5-kip Truck Axle Loading Position 2	0.013	0.003	0.001	0.004	23	8	31
33.2-kip Truck Axle Loading Position 2	0.022	0.006	0.002	0.008	27	9	36
60-kip Load Cart Loading Position 2	0.029	0.008	0.002	0.010	28	7	34
100-kip Load Cart Loading Position 2	0.050	0.016	0.005	0.021	32	10	42

TABLE 15.--COMPARISON OF MEASURED SUBGRADE MOVEMENT WITH THEORETICAL DEFLECTION, STATIC LOAD TESTS EAST SECTION

Load	Theoretical Total Deflection in. k = 500	Average Measured Displacement in.			Percent of Theoretical Total Deflection		
		13-23 in.	23-29 in.	13-29 in.	13-23 in.	23-29 in.	13-29 in.
19.5-kip Truck Axle Loading Position 1	0.010	<0.001	<0.001	<0.001			
33.2-kip Truck Axle Loading Position 1	0.015	0.001	0.001	0.002	7	7	13
60-kip Load Cart Loading Position 1	0.021	0.003	0.001	0.004	14	5	19
100-kip Load Cart Loading Position 1	0.035	0.006	0.002	0.008	17	6	23
19.5-kip Truck Axle Loading Position 2	0.010	--	--	--			
33.2-kip Truck Axle Loading Position 2	0.015	<0.001	<0.001	<0.001			
60-kip Load Cart Loading Position 2	0.021	0.003	0.001	0.004	14	5	19
100-kip Load Cart Loading Position 2	0.035	0.005	0.003	0.008	14	9	23

TABLE 16.--COMPARISON OF MEASURED DISPLACEMENTS WITH THEORETICAL DISPLACEMENTS FOR 13- TO 29-IN. DEPTH

Load kips	Location	Truck				Load Cart			
		Average Displacement, in.		Theoretical Displacement, in.		Average Displacement, in.		Theoretical Displacement, in.	
		Loading Position 1	Loading Position 2	Loading Position 1	Loading Position 2	Loading Position 1	Loading Position 2	Loading Position 1	Loading Position 2
19.5	West Slab	0.005	0.004	0.0048	0.0044				
33.2	West Slab	0.008	0.008	0.0081	0.0075				
60.0	West Slab					0.011	0.010	0.0118	0.0135
100.0	West Slab					0.023	0.021	0.0197	0.0225
19.5	East Slab	<0.001	--	0.0018	0.0012				
33.2	East Slab	0.002	<0.001	0.0031	0.0021				
60.0	East Slab					0.004	0.004	0.0037	0.0036
100.0	East Slab					0.008	0.008	0.0062	0.0060

TABLE 17.--THEORETICAL HORIZONTAL STRESS AND STRAIN PARALLEL TO PAVEMENT EDGE

Loading Condition	West Section				East Section			
	Theoretical Stress, psi		Theoretical Strain, 10^{-4} in./in.		Theoretical Stress, psi		Theoretical Strain, 10^{-4} in./in.	
	Top of Pavement	Bottom of Pavement	Top of Pavement	Bottom of Pavement	Top of Pavement	Bottom of Pavement	Top of Pavement	Bottom of Pavement
19.5-kip Truck Axle Loading Position 1	-282	+279	-0.5	+0.5	-214	+211	-0.4	+0.4
33.2-kip Truck Axle Loading Position 1	-472	+467	-0.8	+0.8	-358	+353	-0.6	+0.6
60-kip Load Cart Loading Position 1	-425	+407	-0.7	+0.7	-311	+291	-0.5	+0.5
100-kip Load Cart Loading Position 1	-708	+678	-1.1	+1.1	-518	+485	-0.8	+0.8
19.5-kip Truck Axle Loading Position 2	-136	+132	-0.2	+0.2	-69	+64	-0.2	+0.2
33.2-kip Truck Axle Loading Position 2	-233	+225	-0.5	+0.5	-117	+109	-0.3	+0.3
60-kip Load Cart Loading Position 2	-125	+120	-0.2	+0.2	+11	-17	+0.05	-0.06
100-kip Load Cart Loading Position 2	-208	+200	-0.3	+0.3	+18	-28	+0.08	-0.10

Note: + denotes tension; - denotes compression.

TABLE 18.--COMPARISON OF MEASURED HORIZONTAL SUBGRADE STRAIN WITH THEORETICAL HORIZONTAL SUBGRADE STRAIN

Loading Condition	West Section				East Section			
	Parallel to Edge at 18-in. Depth		Perpendicular to Edge at 18-in. Depth		Parallel to Edge at 18-in. Depth		Perpendicular to Edge at 18-in. Depth	
	Measured Strain 10^{-4} in./in.	Theoretical Strain 10^{-4} in./in.	Measured Strain 10^{-4} in./in.	Theoretical Strain 10^{-4} in./in.	Measured Strain 10^{-4} in./in.	Theoretical Strain 10^{-4} in./in.	Measured Strain 10^{-4} in./in.	Theoretical Strain 10^{-4} in./in.
19.5-kip truck axle loading position 1	+6	+1.0	+7	+0.6	+4	+0.5	+5	+0.3
33.2-kip truck axle loading position 1	-1	+1.7	-1	+1.0	-3	+0.9	+3	+0.5
60-kip load cart loading position 1	-1	+1.5	+1	+1.6	<1	+0.7	+3	+0.7
100-kip load cart loading position 1	+5	+2.5	-2	+2.7	+1	+1.2	+3	+1.2
19.5-kip truck axle loading position 2	+4	+0.9	<1	+0.1		+0.4		-0.1
33.2-kip truck axle loading position 2	+1	+1.5	+2	+0.1	-2	+0.7	+1	-0.2
60-kip load cart loading position 2	-1	+1.1	+1	+1.8	+3	+0.2	+3	+0.6
100-kip load cart loading position 2	-2	+1.8	+2	+3.0	+3	+0.3	+3	+1.0

Note: + denotes tension; - denotes compression.

TABLE 19.--VERTICAL STRESSES AT BOTTOM OF PAVEMENT
EAST AND WEST SECTIONS, STATIC LOAD TESTS

Loading Condition	Measured Vertical Stress at Bottom of West Section psi	Theoretical Vertical Stress at Bottom of West Section psi	Measured Vertical Stress at Bottom of East Section psi	Theoretical Vertical Stress at Bottom of East Section psi
19.5-kip truck axle loading position 1	2	2.5	3	4.1
33.2-kip truck axle loading position 1	4	4.3	5	6.9
60-kip load cart loading position 1	--	5.7	2	8.0
100-kip load cart loading position 1	--	9.5	4	13.3

Note: Load cart tests were conducted 9 months after truck tests.

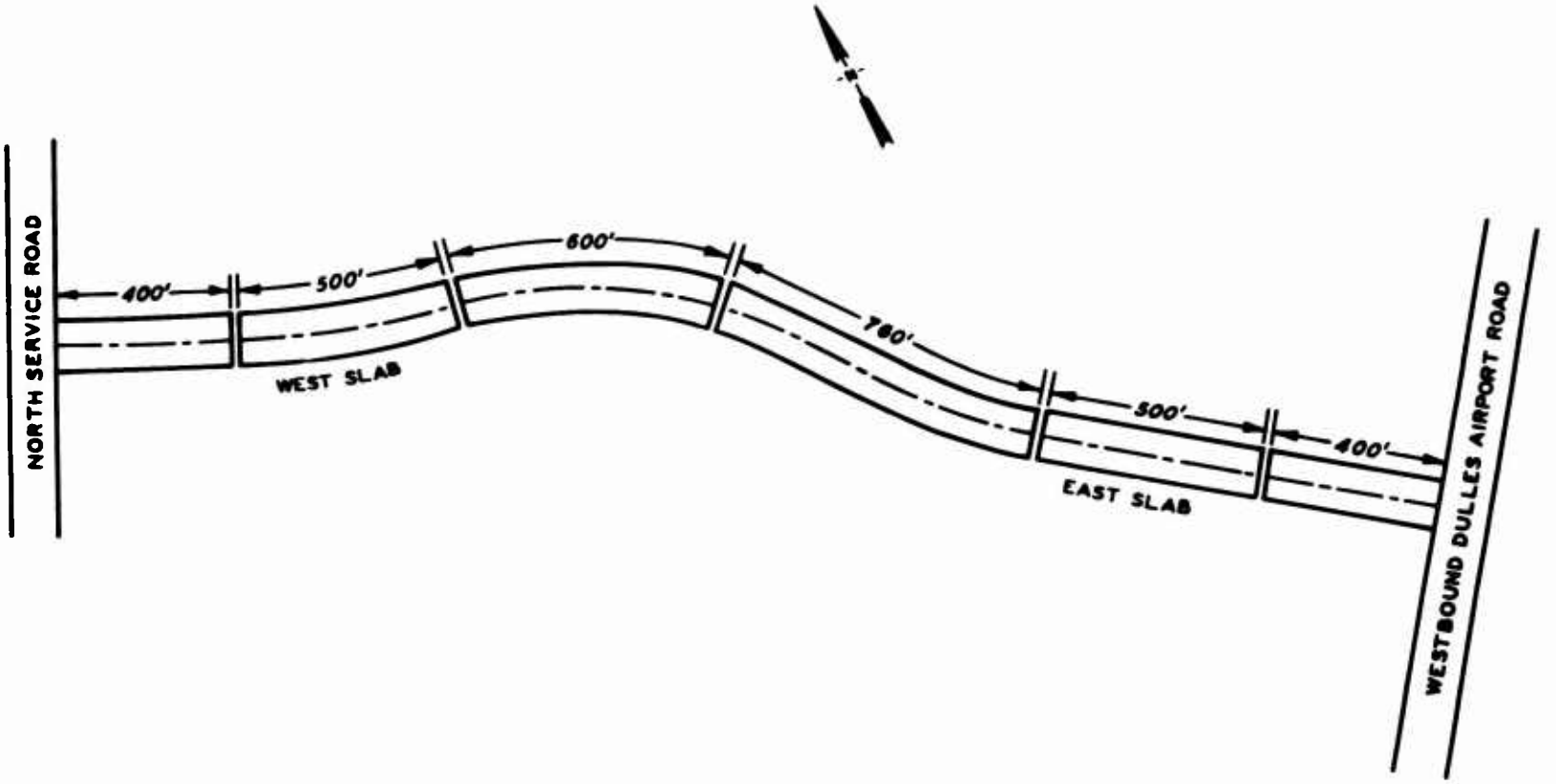

Figure 1. General layout of test road

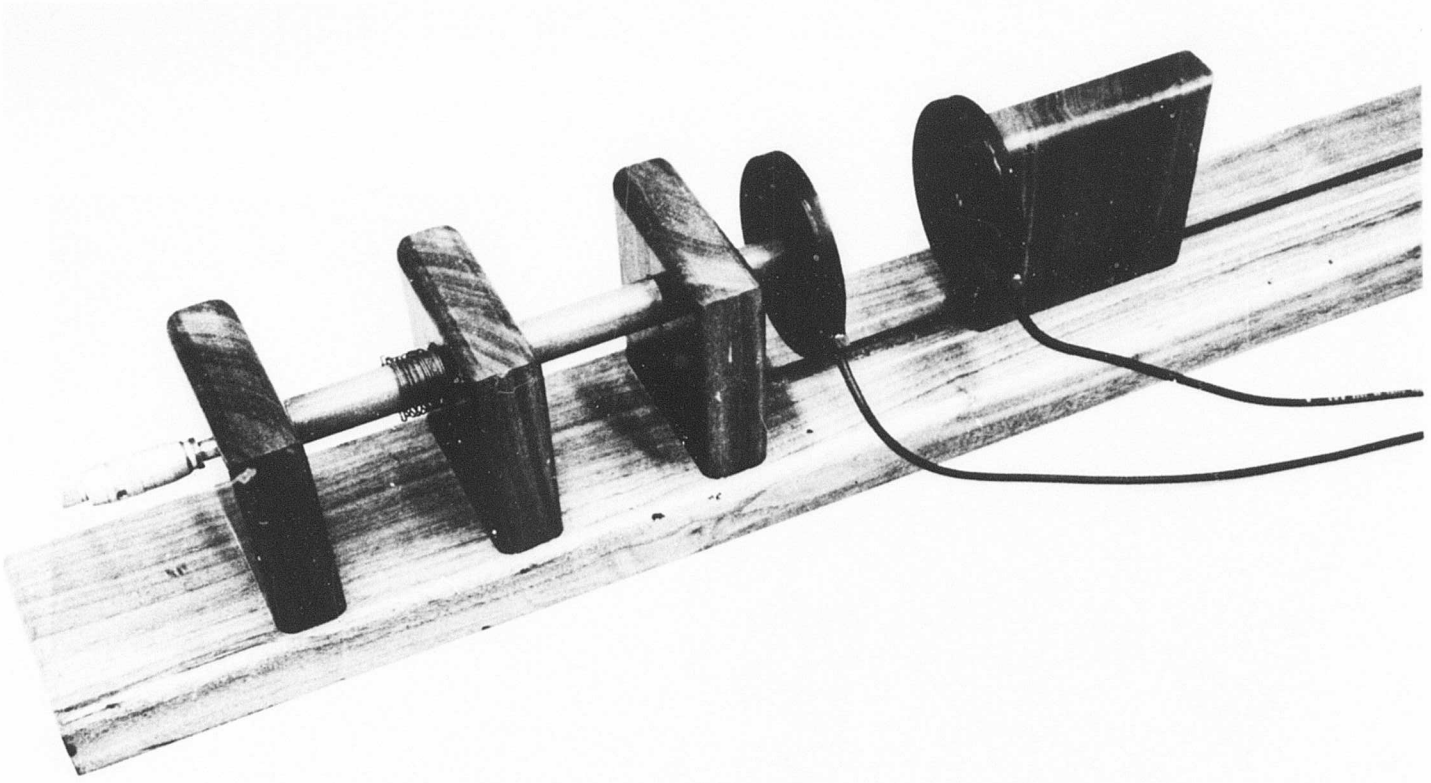

Figure 2. Two 4-in.-diam Bison coils in a micrometer calibration mount

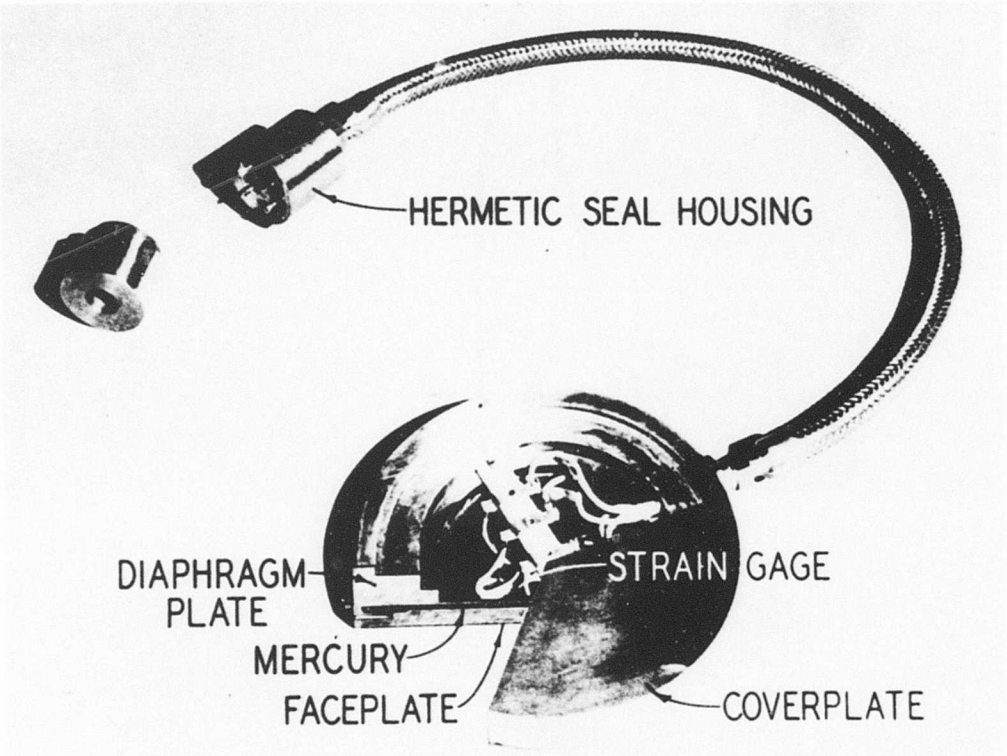

a. WES cell

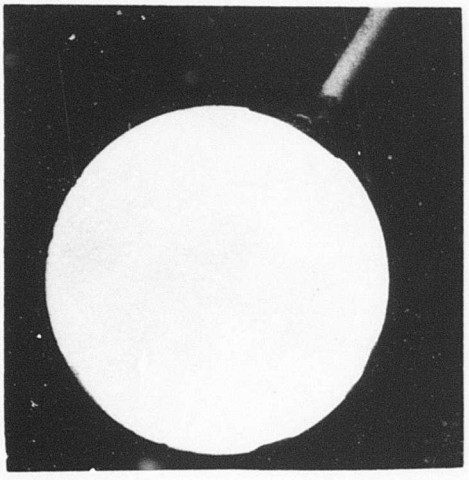

b. URS cell

Figure 3. Soil pressure cells

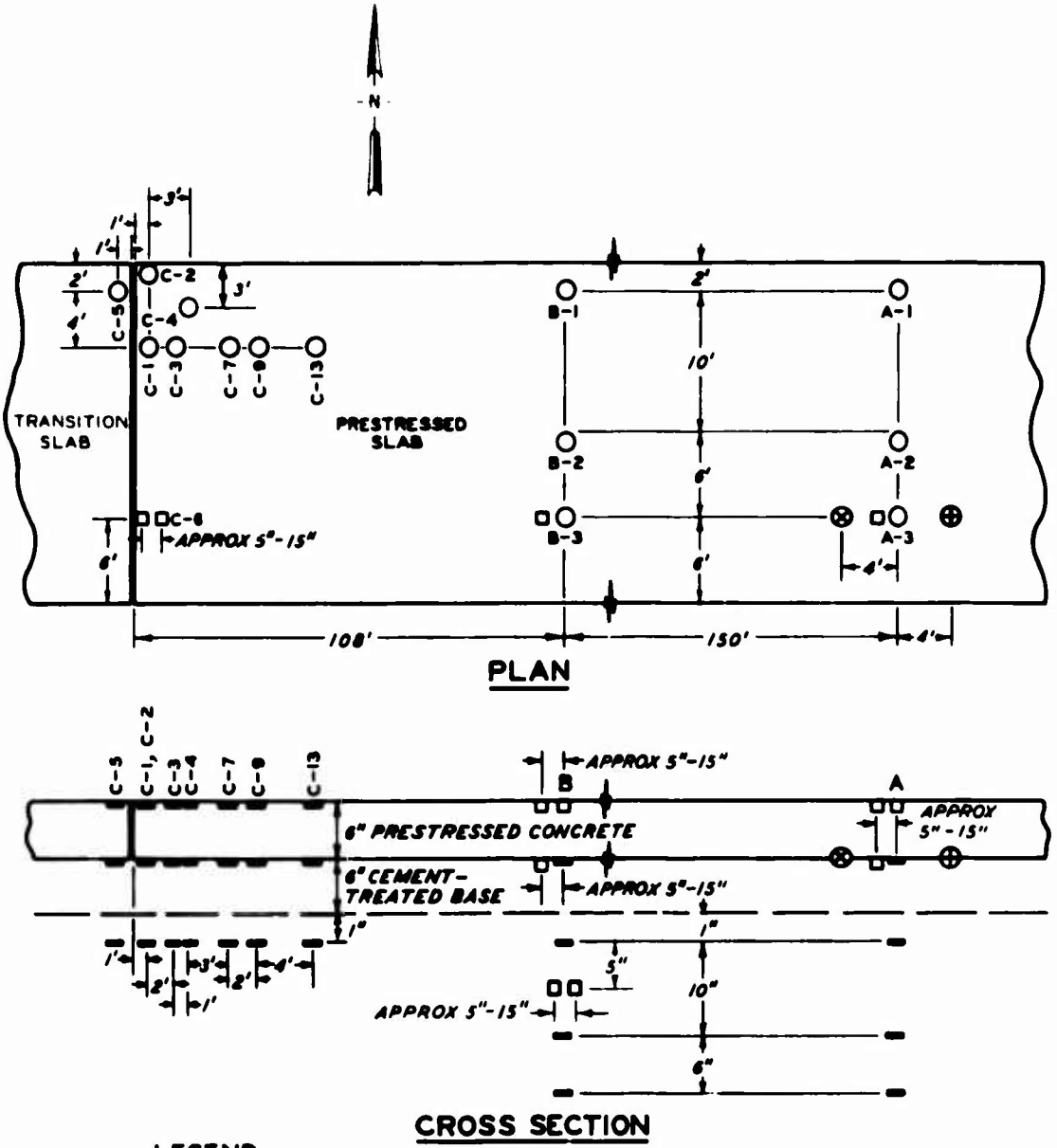

Figure 4. Instrumentation placement in east slab (test section)

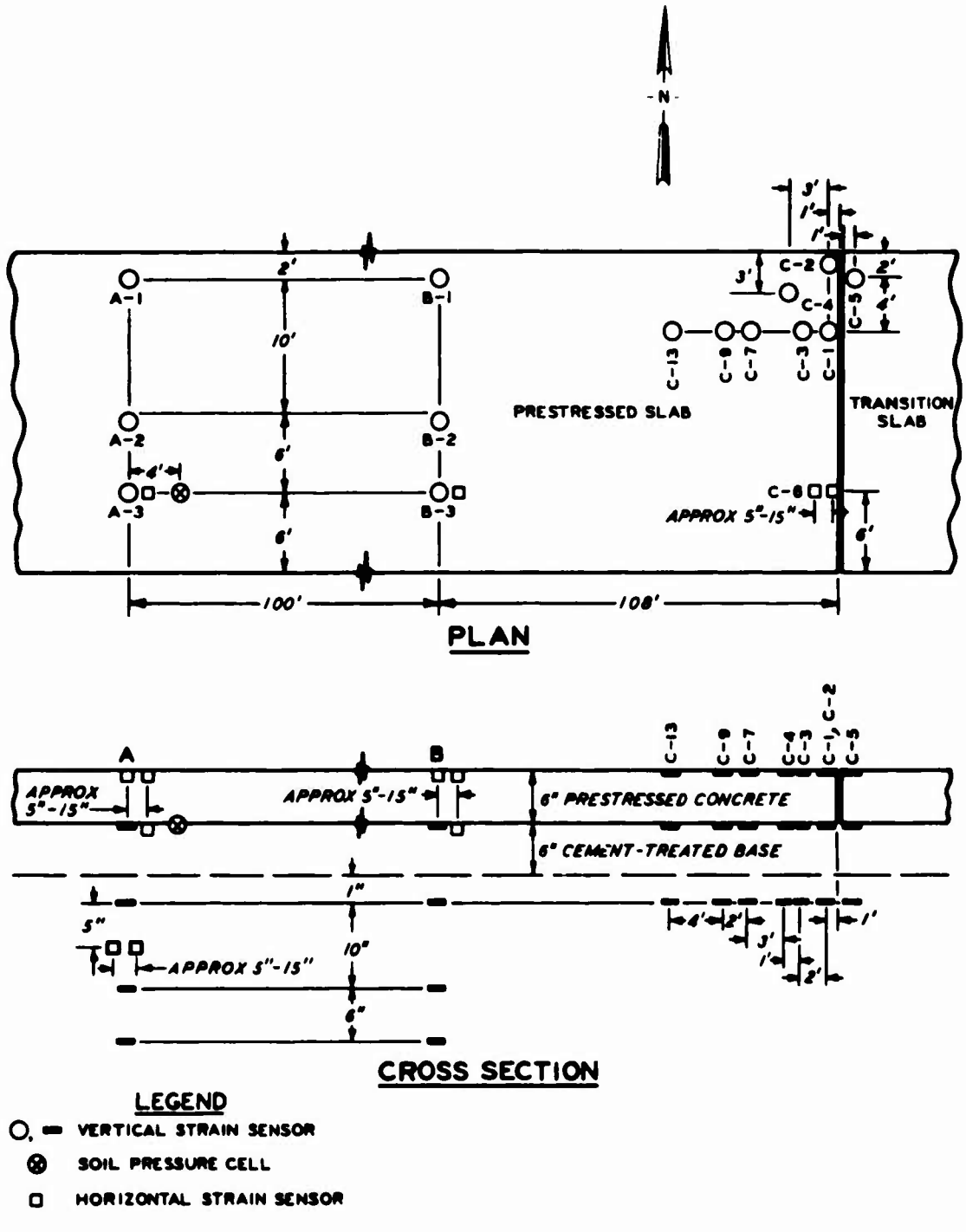

Figure 5. Instrumentation placement in west slab (test section)

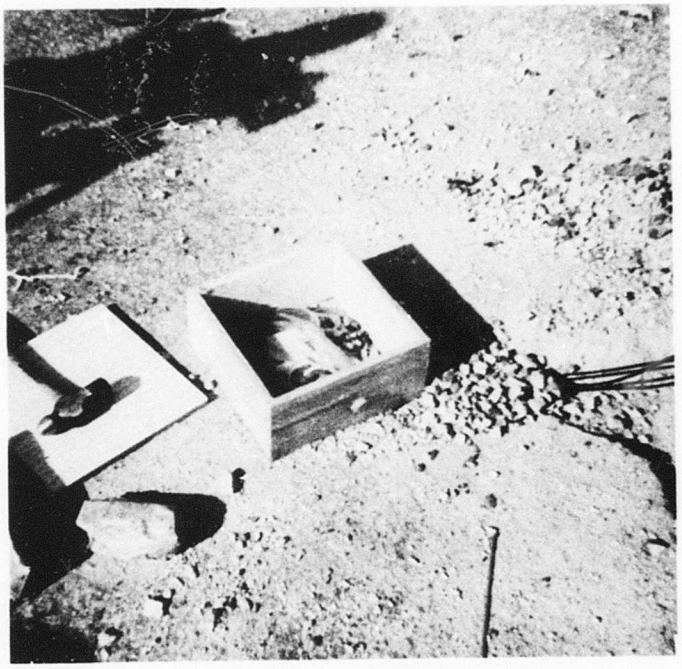

Figure 6. Removable forms used for installation of strain sensors

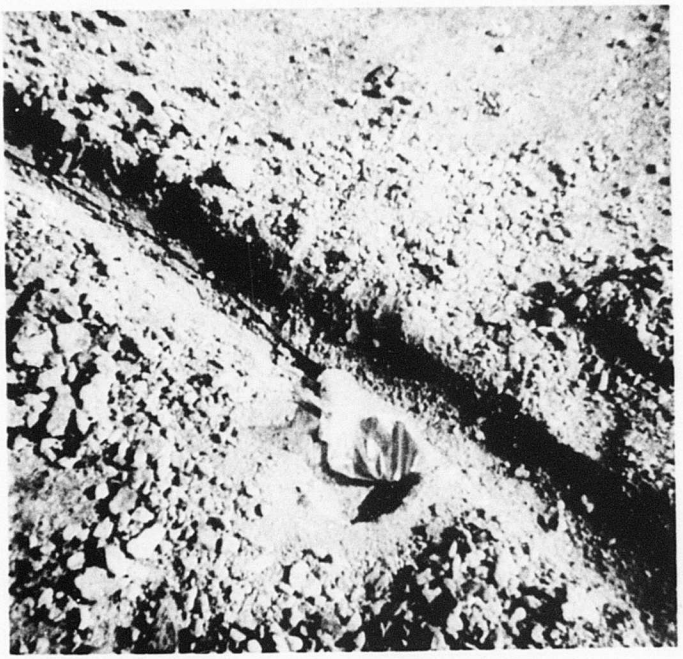

Figure 7. Strain sensor in waterproof bag

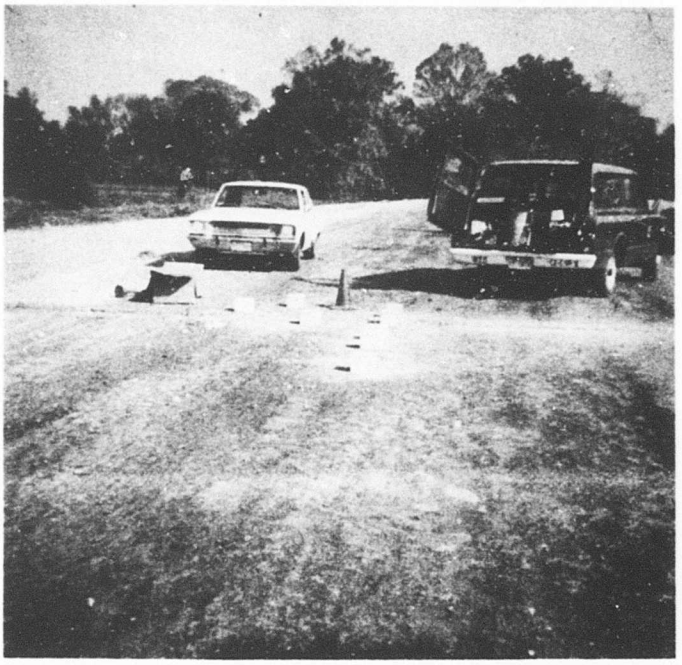

Figure 8. Strain gage pattern at joint

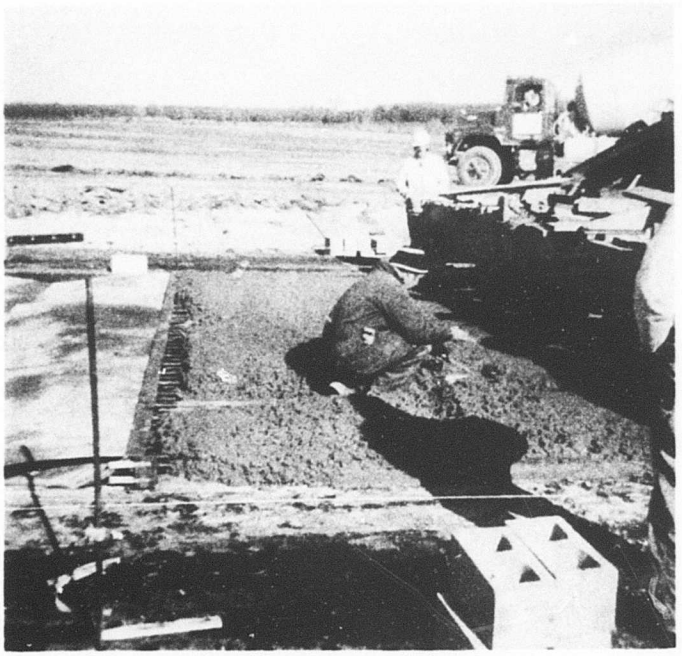

Figure 9. Strain sensor being checked during paving operation

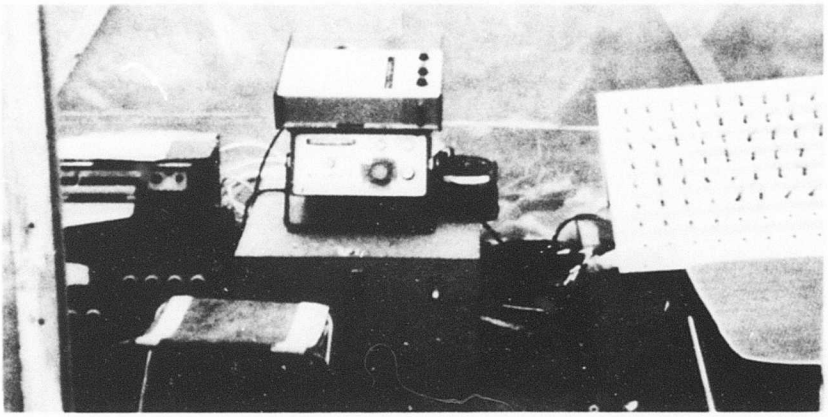

Figure 10. Recording instruments for strain sensors

Figure 11. Truck used for load tests

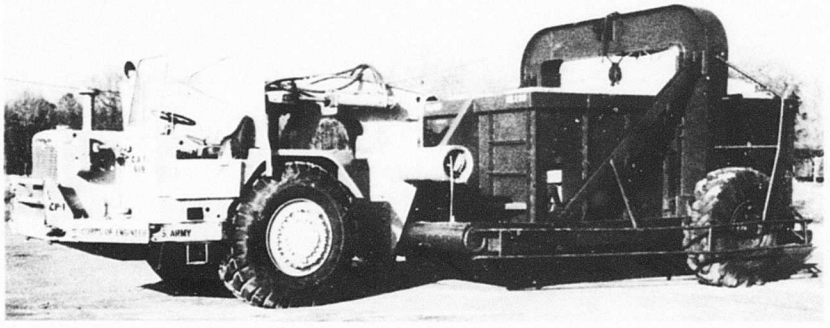

Figure 12. Load cart used for load tests

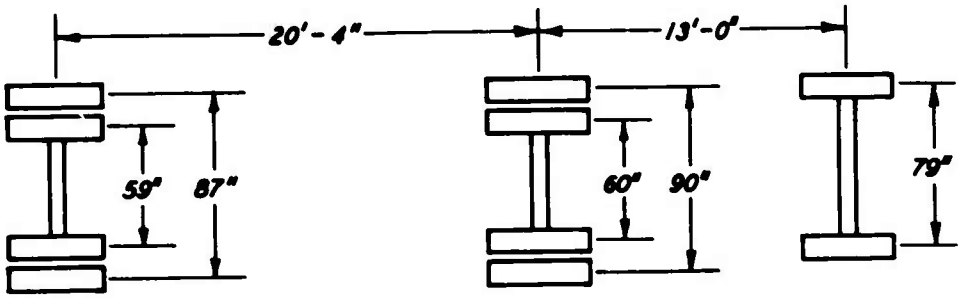

a. Test truck

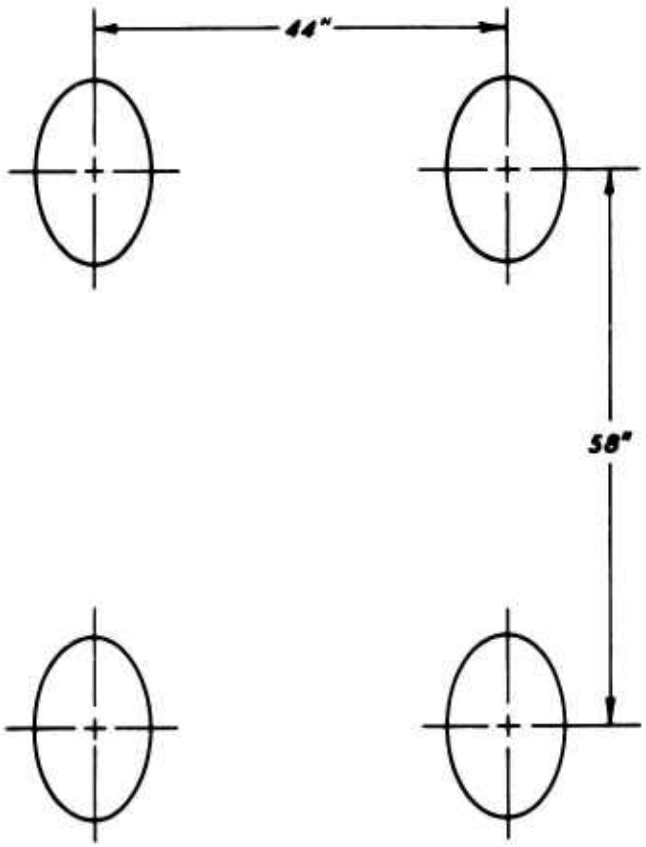

b. Dual-tandem aircraft gear

Figure 13. Tire and axle spacings

a. Truck tests

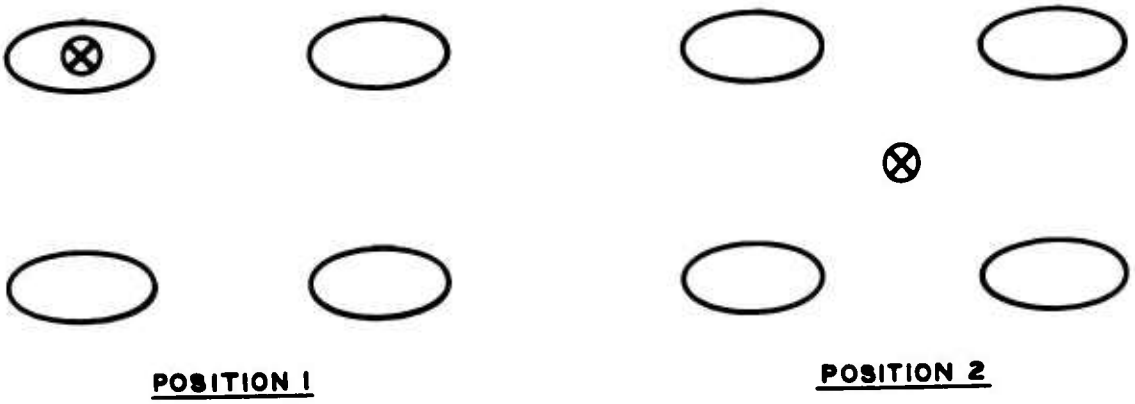

b. Load cart tests

Figure 14. Primary loading positions

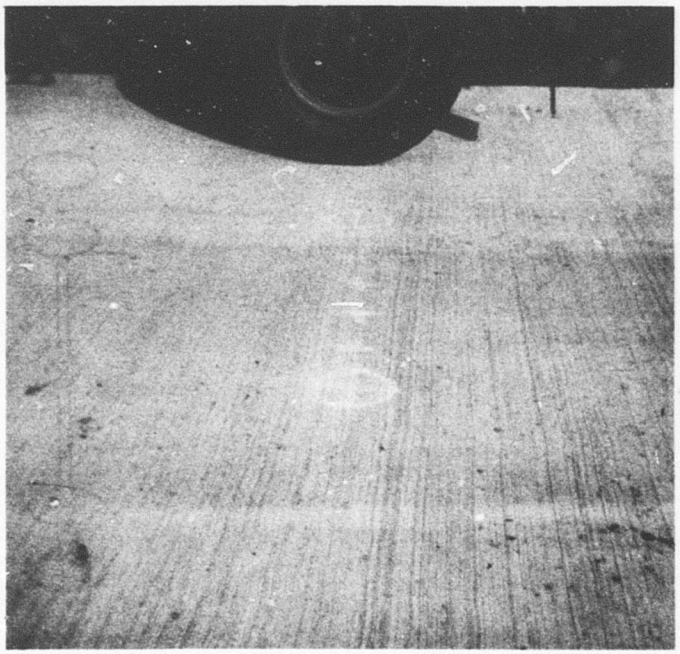

Figure 15. Typical truck load test

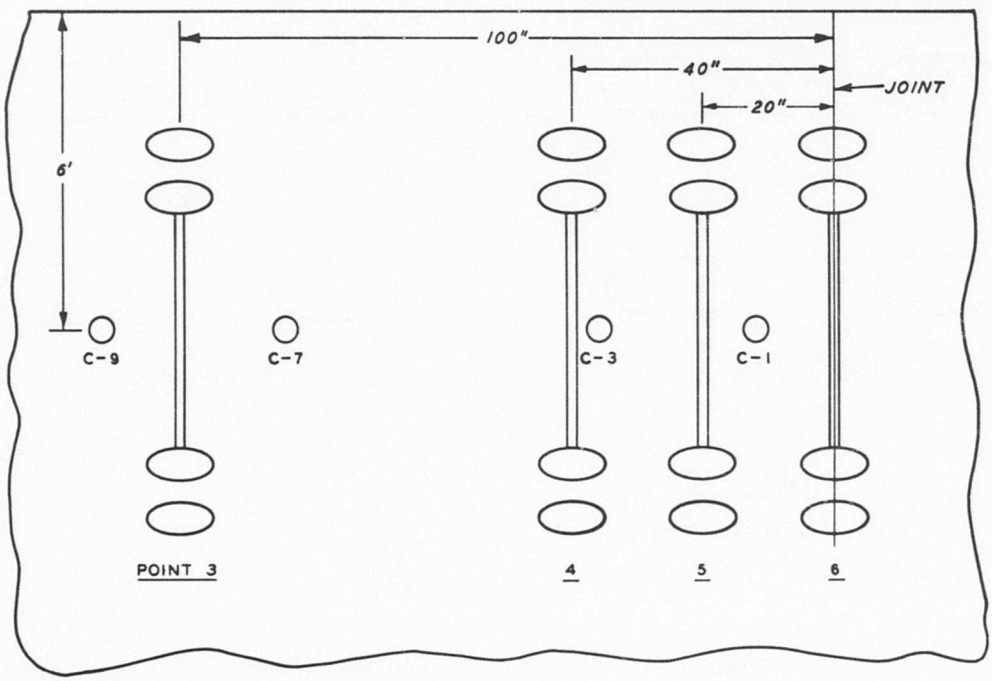

Figure 16. Additional loading points for truck tests

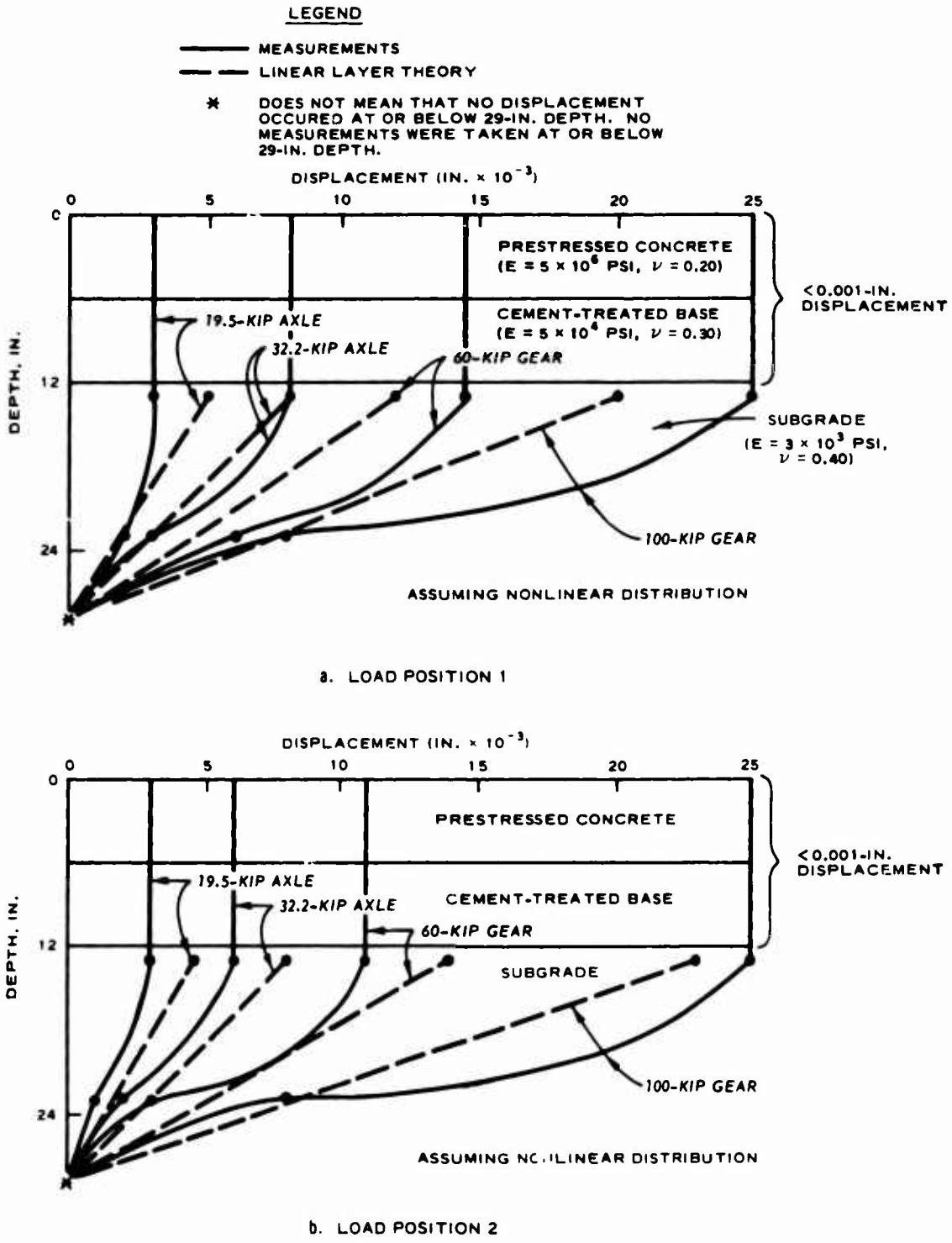

Figure 17. Typical displacement versus depth, point B-3 west test section

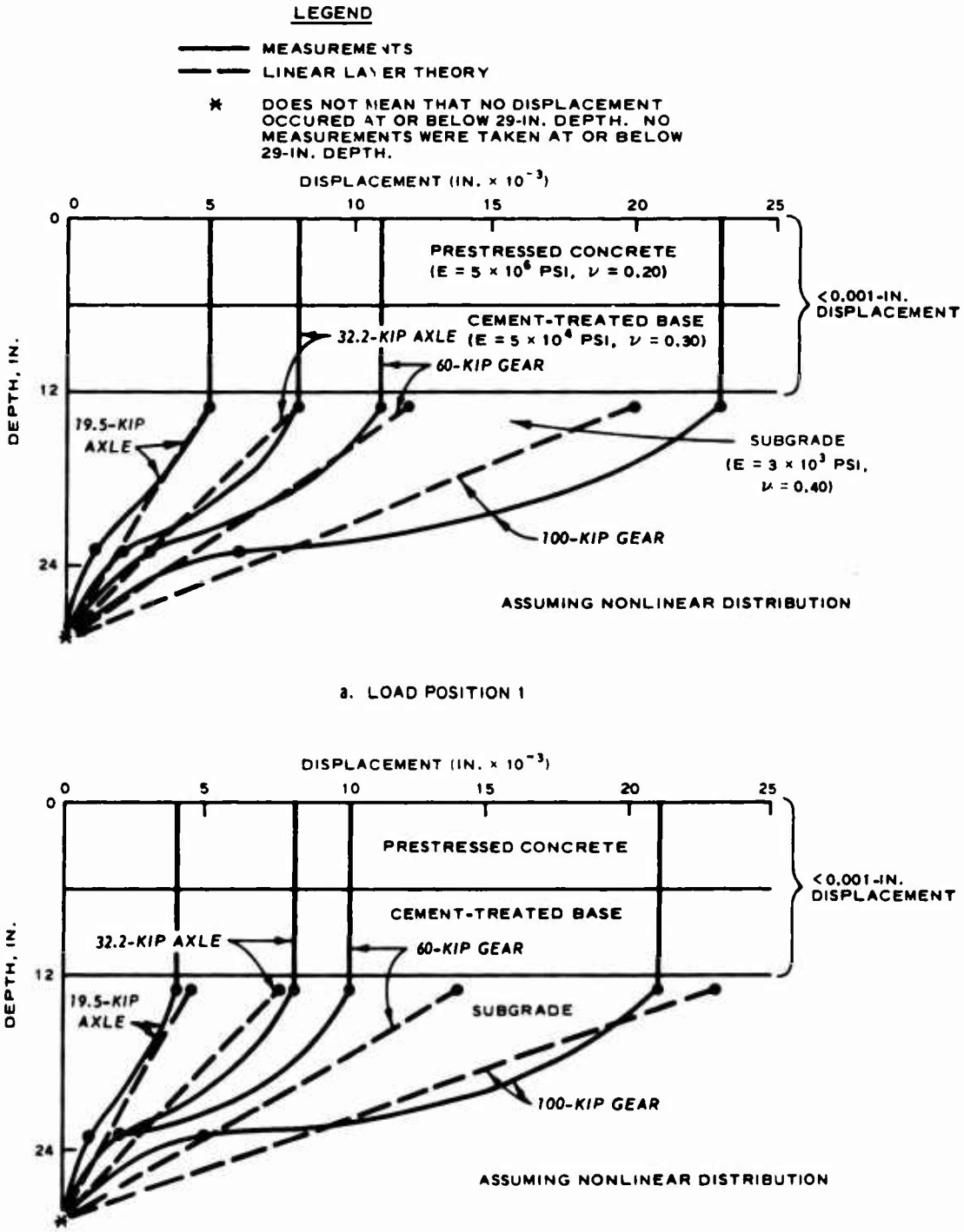

Figure 18. Average displacement versus depth, west test section

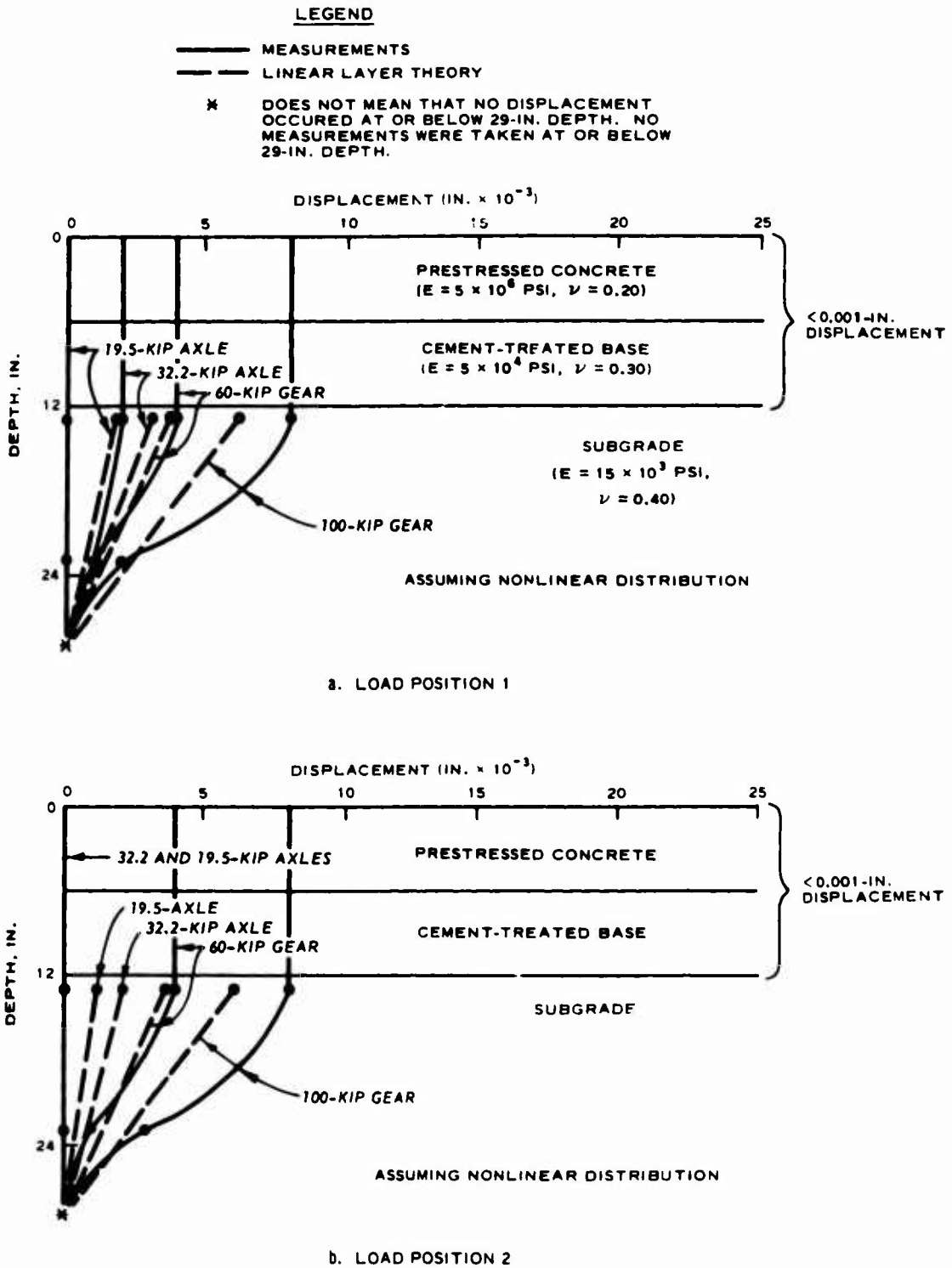

Figure 19. Average displacement versus depth, east test section

REFERENCES

1. Friberg, B. F. and Pasko, T. J., Jr., "Prestressed Concrete Highway Pavement at Dulles International Airport: Research Progress Report to 100 Days," Report No. FHWA-RD-72-29, Aug 1973, Federal Highway Administration, Office of Research, Washington, D. C.

2. Federal Highway Administration, "Final Report, Prestressed Concrete Pavement Construction," Report No. FHWA-RDDP-17-1, Feb 1973, Washington, D. C.

3. American Association of State Highway Officials, "Recommended Practice for the Classification of Soils and Soil-Aggregate Mixtures for Highway Construction Purposes," Designation: M 145-66, Standard Specifications for Highway Materials and Methods of Sampling and Testing, Part I, 1970, Washington, D. C.

4. Federal Aviation Administration, "Airport Paving," Advisory Circular AC 150/5320-6A, Sep 1971, Washington, D. C.

5. Burns, C. D., Ledbetter, R. H., and Grau, R. W., "Study of Behavior of Bituminous-Stabilized Pavement Layers," Miscellaneous Paper S-73-4, Mar 1973, U. S. Army Engineer Waterways Experiment Station, CE, Vicksburg, Miss.

6. Bison Instruments, Inc., "Instruction Manual, Bison Instruments Soil Strain Gage Model 4101 A," Minneapolis, Minn.

7. Ledbetter, R. H. et al., "Multiple-Wheel Heavy Gear Load Pavement Tests; Presentation and Initial Analysis of Stress-Strain-Deflection and Vibratory Measurements; Instrumentation and Data and Analysis," Technical Report S-71-17, Vol IIIA and Vol IIIB, Nov 1971, U. S. Army Engineer Waterways Experiment Station, CE, Vicksburg, Miss.

8. Woodman, E. H., "Pressure Cells for Field Use," Bulletin No. 40, Jan 1955, U. S. Army Engineer Waterways Experiment Station, CE, Vicksburg, Miss.

9. Walker, D., Kriebel, A. R., and Kaplan, K., "URS Free Field Soil Stress Gauge: Design, Construction and Evaluation," URS 758-6, Feb 1971, URS Research Company, San Mateo, Calif.

10. Odom, E. C. and Carlton, P. F., "Prestressed Concrete Pavements; Design and Construction Procedures for Civil Airports," Technical Report FAA-RD-74-34-II, Vol II (in preparation), Federal Aviation Administration, Washington, D. C.

11. Pickett, G. and Ray, G. K., "Influence Charts for Concrete Pavements," Transactions, American Society of Civil Engineers, Vol 116, No. 2425, 1951, p 49.

12. Peutz, M. G. F., Kempen, H. P. M. van, and Jones, A., "Layered Systems Under Normal Surface Loads," Soil Stresses and Pavement Element Analyses, Highway Research Record 228, pp 34-45, 1968, Highway Research Board, National Academy of Sciences - National Academy of Engineering, Washington, D. C.